PhD degree in Molecular Medicine (curriculum in Molecular Oncology)

European School of Molecular Medicine (SEMM),

University of Milan and University of Naples "Federico II"

Settore disciplinare: MED/04

Non-genetic mechanisms of chemoresistance in acute myeloid leukemia

Sara Milovanović

European Institute of Oncology (IEO), Milan

Matricola n.R12428

Supervisor: Prof. Pier Giuseppe Pelicci, MD, PhD European Institute of Oncology (IEO), Milan

Added Supervisors: Dr. Thalia Vlachou, PhD
European Institute of Oncology (IEO), Milan

Dr. Emanuela Colombo, PhD
European Institute of Oncology (IEO), Milan

Ph.D. Coordinator: Prof. Saverio Minucci

Academic year 2021-2022

Acknowledgments

To acknowledge first those who gave the most for this project, I would have to go for a rather unusual choice. I would like to give all my admiration and respect to 202 mice who gave their lives for this project to succeed, I believe they should be remembered for their contribution to science.

The next most important person to thank would be my principal investigator and my mentor, Pier Giuseppe Pelicci. I would like to thank him for sharing his brilliant ideas in order to teach me how to see deeper and further into the future. Finally, I want to thank him for showing me what science really is and how playful our minds need to be to create the path to great discoveries.

I would like to thank my supervisor and friend Thalia Vlachou, for leading me for many years, and helping me professionally and personally. I will always remember those long evenings and nights spent running to meet the deadlines, funny life stories and those hedonist breaks tasting the best drinks from all over the world.

The next would be, of course, Simone Frascolla (Fragola), my Ph.D. child. I would like to thank him for making science fun, making every moment fun, and always seeing the bright side of the story!

The baby of our team, Giulia Perticari, I would like to thank for all the help and new ideas that she brought to our project.

I would also like to thank other members of the PGP group, FACS facility, Genomic unit, Imaging unit, Molpath, and Cogentech staff for all the help throughout the years.

On the other side of the coin, I would like to thank Amir, Anjali, Goga, Angeli, Johannes, Catiana, Eirini and Iman for being my support in my personal life and for sharing life in Italy for 4 years.

My family, I want to thank for me being me, for creating this person who is writing this now. Thanks to my father, Saša, I got a bit of crazy genetics to always try something new. My brothers, Luka and Matej, thought me how to fight for myself and they were always my support in life. Special thanks to my mother, Ljiljana, who gave me this life and survived so many battles for me to reach this point.

I would like to thank all my friends back home, for making it my home, and those out of Serbia, for making the world my home.

My husband, Yazan, I would like to thank for being there through the world pandemic, and many other moments, and for giving me the best gift I could get.

Last, because you arrived the last, my miracle of life, my son, Gabriel, I want to thank for giving my life a new meaning and new path!

Table of Contents

List of Figures

List of tables

List of abbreviations

ALL	Acute lymphoblastic leukemia
AML	Acute myeloid leukaemia
AraC	Cytarabine arabinoside
ASXL1	Additional Sex Comb-Like 1
BFP	Blue fluorescent protein
BM	Bone marrow
BrdU	Bromodeoxyuridine
BSA/PBS	Bovine serum albumin in PBS
CE	Clonal evolution
CEBPA	CCAAT Enhancer binding protein □
CLL	Chronic lymphocytic leukemia
CML	Chronic myeloid leukemia
CR	Complete remission
CSC	Cancer stem cell
DEPTH	Deviating gene Expression Profiling Tumor Heterogeneity
DMSO	dimethyl sulfoxide
DNMT3a	DNA Methyltransferase 3A
Doxo	Doxorubicin
EDTA	Ethylenediaminetetraacetic acid
ELDA	Extreme limiting dilution analysis
ELN	European LeukemiaNet
FACS	Fluorescence activated cell sorting
FBS, NA	Foetal bovine serum, North-American
FBS, SA	Foetal bovine serum, South-American
FLAG-IDA	Fludarabine and G-CSF for modified IDAC
IRENA lnc	
RNA	Long noncoding RNA IFN-responsive nuclear factor-κB activator
FLT3	Fms-like Tyrosine Kinase
FLT3-ITD	Fms-like Tyrosine Kinase-Isocitrate Dehydrogenase
GBC	Guide barcodes
GFP	Green fluorescent protein
GO	Gemtuzumab Ozogamicin
GO terms	Gene ontology terms

H2B	Histone 2B
HCT	Hematopoietic cell transplantation
hMSC	Human mesenchymal cells
HSC	Hematopoietic stem cell
IC50	Half maximal inhibitory concentration
IDAC	Idarubicin with Cytarabine
IFN	Interferon
IP	Intraperitoneal
IRDS	IFN-related DNA damage resistance signature
ITD	Isocitrate Dehydrogenase
ITH	Intratumor heterogeneity
KEGG	Kyoto Encyclopedia of Genes and Genomes
LB	Luria-Bertani
LIC	Leukaemia initiating cell
LR	Label retaining
LSC	Leukemia stem cell
MDS	Myelodysplastic syndrome
MEC	Mitoxantrone, Etoposide and Cytarabine
MOI	Multiplicity of infection
MPN	Myeloproliferative neoplasms
NPM1	Nucleolar protein nucleophosmin 1
NSG	NOD SCID IL2RG null
PB	Peripheral blood
PDX	Patient derived xenograft
PFA	Paraformaldehyde
PM	Plasma membrane
PuroR	Puromycin resistance marker
RBC	Red blood cell
RRE	Rev response element
RUNX1	Runt-related transcription factor
scRNAseq	Single-cell RNA sequencing
SPL	Spleen
TAE	Tris-acetate-EDTA buffer
TAM	Tumor-associate macrophages
TET2	Ten-Eleven Translocation 2

TIC	Tumor intitating cell
US	United States
VSV-G	Vesicular stomatitis virus protein G
WES	Whole exome sequencing
WHO	World Health Organisation

Abstract

Acute Myeloid Leukemia (AML) is the most common type of acute hematological malignancy in adults. 40–60% of patients relapse due to the emergence of cellular resistance to anti-leukemic drugs. Drug resistance in leukemic cells has been associated with intratumoral heterogeneity, among which quiescence, specifically, is considered a key factor for cell survival. Currently, experimental evidence collected both from patients and model systems suggests that relapse is due to rare persistent AML cells which survive chemotherapy. These chemotherapy persistent cells are not yet biologically and molecularly defined. Open questions are whether persistent cells are drug-resistant, what are their cellular and molecular features, as well as their content in leukemic stem cells (LSCs). My *working hypothesis* is that chemoresistance in AMLs is associated with specific phenotypic states that characterize rare cell populations found within the pool of quiescent leukemic cells. These cells are selected by chemotherapy and represent the cellular basis of the relapse. In order to test my hypothesis, I explored transcriptional and functional characteristics of quiescent leukemic cells and tested the effect of chemotherapy. Here, I present two newly established xeno-models of chemoresistant human AMLs that closely recapitulate clinical data. My data show that quiescent cells accumulate over time and that quiescence is not a stable state; instead quiescent and proliferating cells can switch from one state to another. Notably, quiescent cells are selectively spared by chemotherapy and show resistance to additional rounds of treatment. Finally, quiescent cells appear as the only carrier of tumorigenic capacity in AMLs and are, therefore, deemed essential for leukemia development and, possibly, relapse.

1 Introduction

1.1 Leukemia epidemiology, clinical representation, and classification

Cancer represents a large group of diseases that can occur in almost any organ or tissue of the human body; they are characterized by the uncontrollable growth of abnormal cells and the capability of spreading to other organs. In most cases, cancer is the result of a multi-stage process leading to the transformation of normal tissue into a precancerous lesion and, eventually, a malignant tumor[1]. Based on estimates from the World Health Organization (WHO), cancer is within the top two causes of death in people younger than 70 years in 112 out of 183 countries[2]. In 2020, 19.3 million new cancer cases and almost 10 million cancer deaths were observed worldwide[3]. In Europe, it was estimated that 4 million new cases and 1.9 million cancer deaths occurred in 2020[4], while the estimated number of new cases in 2021 in the United States (US) was 1.9 million with 600,000 cancer deaths[5]. Five-year relative survival was estimated to be 67.7% (based on data from 2011-2017 in the US)[5]. The median age of cancer patients at diagnosis was 66 years[5]. By 2040, the cancer burden is expected to reach 28.4 million cases worldwide, which represents a 47% increase compared to the 19.3 million new cases observed in 2020 (Fig. 1). Up to date, cancer represents one of the diseases with the highest expansion rates and highest mortality, which makes it one of the most urgent targets for future research.

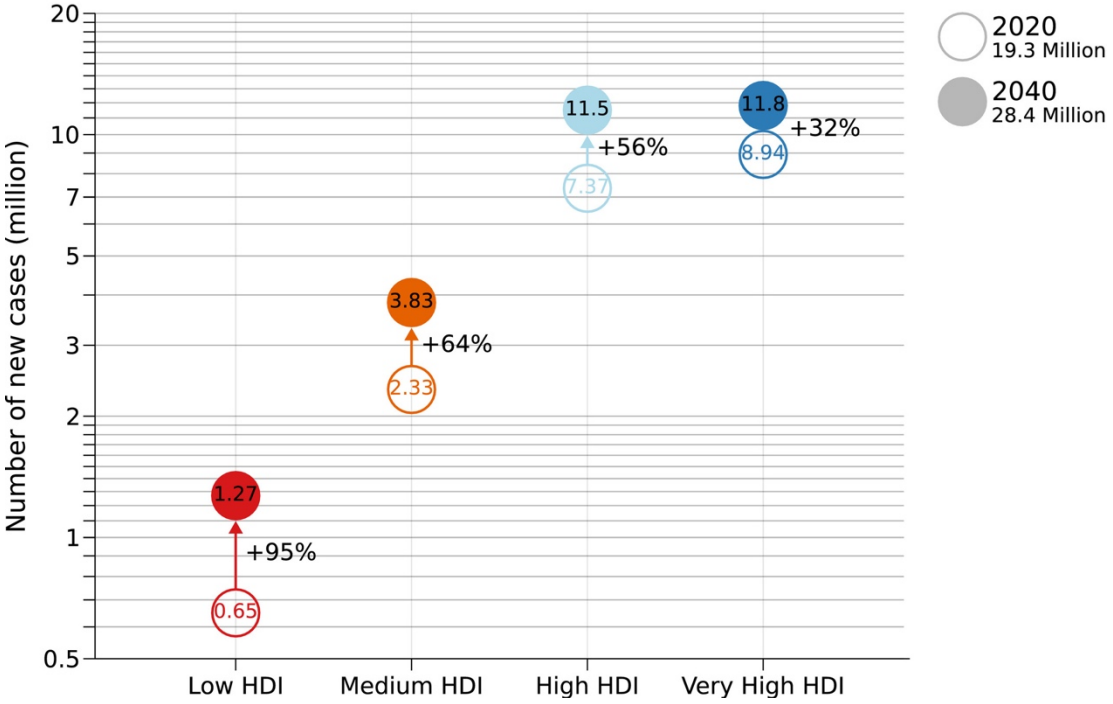

Figure 1. Cancer prediction 2020 to 2040 (adapted from Sung et al.)

Projected number of new cases for all cancers combined (both sexes combined) in 2040 according to the 4-Tier Human Development Index (HDI).

Breast cancer in women and lung cancer in men represent the most common cancer types and cancers with the highest mortality worldwide (Fig. 2)[3]. Leukemia incidence is placed as the 10th most abundant cancer in men and 14th in women worldwide, and it is within the top 10 cancers with the highest mortality in both women and men[3]. In 2021, the estimated number of new cases in the US was 61,090 (3.3% of all cancer cases) and leukemia-related deaths were 23,660 (3.9% of all cancer deaths). Five-year relative survival was estimated to be 65% (based on data from 2011-2017 in the US). The median age at diagnosis was 67 years. Leukemia was more prevalent in males and Caucasians than in females and other races[5]. The lack of available treatments and a high percentage of patients resistant to treatment with available medication makes leukemia an unmet medical need.

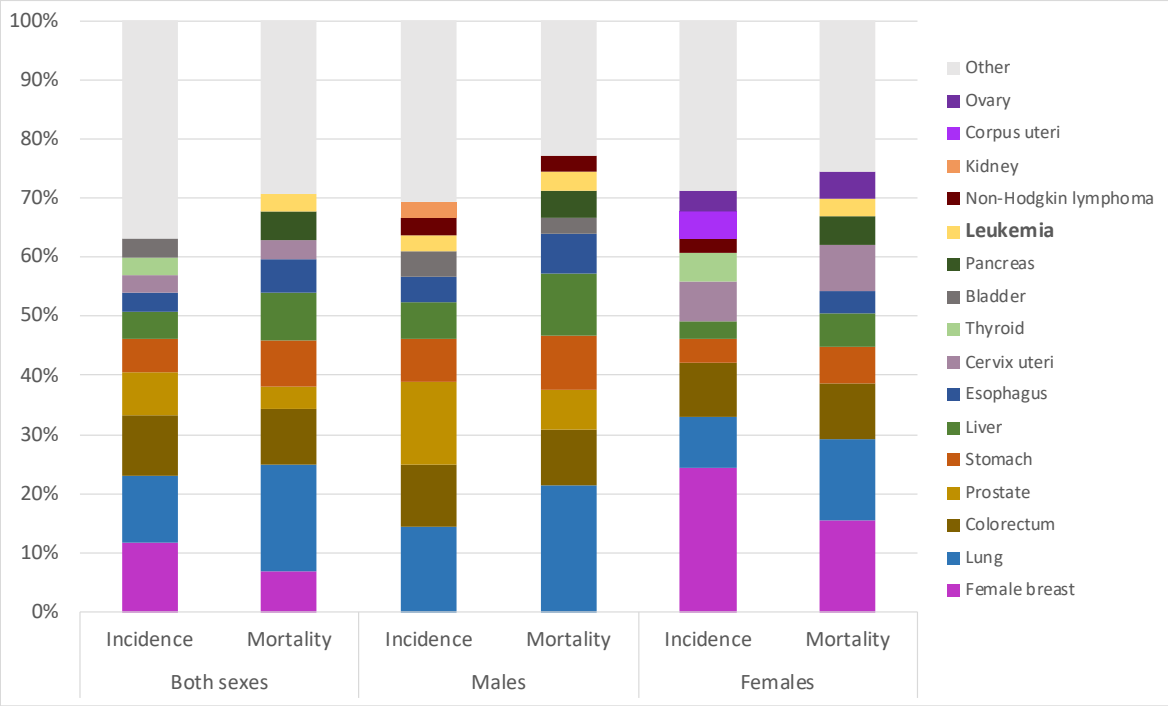

Figure 2. Incidence and mortality of cancer in 2020 worldwide

Relative percentages of each cancer type are shown for both sexes, males only and females only (adapted from Sung et al).

Leukemias are characterized by hyperproliferation of abnormal hematopoietic cells that infiltrate the bone marrow (BM) leading to BM insufficiency (Fig. 3).

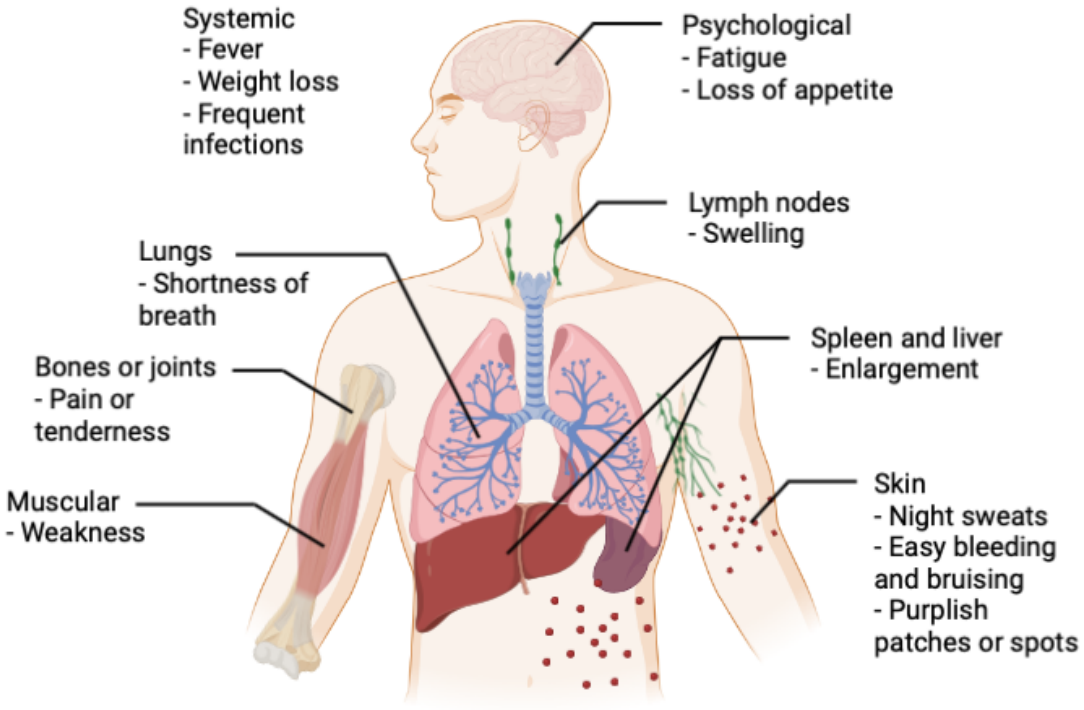

Figure 3. Consequences of BM failure

Consequences of BM failure include signs of leukemia (anemia, thrombocytopenia, and leukopenia), and symptoms of leukemia (frequent infections, fever, difficulties with breathing, muscle weakness, prolonged bleeding, purplish spots on skin, organ enlargement (lymph nodes, liver, spleen (SPL))

Traditionally, leukemias are divided into acute and chronic, lymphocytic and myeloid, and include acute lymphoblastic leukemia (ALL), acute myeloid leukemia (AML), chronic lymphocytic leukemia (CLL), and chronic myeloid leukemia (CML) and other more rare subtypes, like B-cell and T-cell leukemias, and NK cell-related leukemias[6]. Acute leukemias have high numbers of immature and dysfunctional hematopoietic cells (blasts)[6]. Chronic leukemias can go through an accelerated phase, where the number of blasts increases progressively, and transform into acute leukemias.

Based on the new 2016 WHO classification myeloid neoplasms represent a heterogeneous group of diseases that all share phenotypic features of myeloid lineage. They consist of myeloproliferative neoplasms (MPN), which are characterized by hyperproliferation of near normal hematopoietic cells, myelodysplastic syndromes (MDS), which instead show insufficient hematopoiesis and acute myeloid leukemia which has the most aggressive clinical phenotype (AML)[7,8]. Myeloid neoplasms are a continuum, where MPN and MDS represent pre-leukemic syndromes and AML fully developed leukemia.

1.2 Acute Myeloid Leukemia epidemiology and classification

Acute Myeloid Leukemia (AML) is the most common type of acute hematological malignancy in adults[5,9]. It's estimated that AML represents 1.1% of all new cancer cases and 1.9% of all cancer deaths in 2021 (US data)[5]. Like other leukemia types, AML is more prevalent in males and Caucasians than in females and other races. The median age at diagnosis is 68 years. AML has poor survival with 5-year relative survival of only 29.5% (data for 2011-2017)[5].

Based on the latest 2016 revision of the 4th edition of the World Health Organization (WHO) classification of acute myeloid leukemia (AML) and related neoplasms, AML comprises 6 subtypes: AML with recurrent genetic abnormalities, AML with myelodysplasia-related changes, therapy-related myeloid neoplasms, AML not otherwise specified, myeloid sarcoma and myeloid proliferation related to Down syndrome (Table 1)[8].

Table 1. World Health Organization (WHO) classification of acute myeloid leukemia (AML) and related neoplasms (Adapted from Arber et al, Blood, 2016)

AML with recurrent genetic abnormalities
t(8;21)(q22;q22.1); *RUNX1-RUNX1T1*
inv(16)(p13.1q22) or t(16;16)(p13.1;q22); *CBFB-MYH11*
PML-RARA (acute promyelocytic leukaemia, APL)
t(9;11)(p21.3;q23.3); MLLT3-KMT2A
t(6;9)(p23;q34.1); *DEK-NUP214*
inv(3)(q21.3q26.2) or t(3;3)(q21.3;q26.2); *GATA2, MECOM*
t(1;22)(p13.3;q13.3);RBM15-MKL1 (megakaryoblastic AML)
BCR-ABL1 (provisional entity)
mutated *NPM1*
biallelic mutations of *CEBPA*
mutated *RUNX1* (provisional entity)

AML with myelodysplasia- related changes
Complex karyotype (3 or more abnormalities)
Unbalanced abnormalities
-7/del(7q)
del(5q)/t(5q)
i(17q)/t(17p)
-13/del(13q)
del(11q)
del(12p)/t(12p)
idic(X)(q13)
Balanced abnormalities
t(11;16)(q23.3;p13.3)
t(3;21)(q26.2;q22.1)
t(1;3)(p36.3;q21.2)
t(2;11)(p21;q23.3)
t(5;12)(q32;p13.2)
t(5;7)(q32;q11.2)
t(5;17)(q32;p13.2)
t(5;10)(q32;q21.2)
t(3;5)(q25.3;q35.1)
Therapy-related myeloid neoplasms
Therapy-related myelodysplastic syndrome (t-MDS)
Therapy-related AML (t-AML)
AML, not otherwise specified
AML with minimal differentiation
AML without maturation
AML with maturation
Acute myelomonocytic leukaemia
Acute monoblastic/monocytic leukaemia
Pure erythroid leukaemia
Acute megakaryoblastic leukaemia
Acute basophilic leukaemia
Acute panmyelosis with myelofibrosis
Myeloid sarcoma
Myeloid proliferations related to Down syndrome
Transient abnormal myelopoiesis (TAM)
Myeloid leukaemia associated with Down syndrome

AML genetic landscapes have a significant effect on AML prognosis and outcome[10]. Commonly mutated genes in AML which influence AML pathogenesis are subdivided into 8 categories according to their biological function: myeloid transcription-factor genes, NPM1, tumor suppressors, signaling genes, genes involved in the regulation of DNA methylation, chromatin modifier, cohesin complex, and splicing factors (Table 2)[11,12].

Table 2. Categories of commonly mutated genes in AML (adapted from Hou et al, 2020)

Functional category	Gene members	Role in AML Leukemogenesis
Myeloid transcription-factor genes	Transcription factor fusions by chromosomal rearrangements, such as t(8;21)(q22;q22); *RUNX1-RUNX1T1* and inv(16)(p13.1q22) or t(16;16)(p13.1;q22); CBFB-MYH11 GATA2, RUNX1 and CEBPA	Transcriptional deregulation and impaired hematopoietic differentiation.
Nucleophosmin (*NPM1*) gene	*NPM1*	Aberrant cytoplasmic localization of NPM1 and its interacting proteins
Tumor suppressor genes	*TP53, WT1, PHF6*	Transcriptional deregulation and impaired degradation via the negative regulator (MDM2 and PTEN oncogenes)
Signaling genes	*FLT3, KIT, PTPN11, RAS*	Proliferative advantage through the RAS-RAF, JAK-STAT, and PI3K-AKT signaling pathways
DNA methylation	*DNMT3A, TET2, IDH1, IDH2*	Deregulation of DNA methylation and oncometabolite production
Chromatin modifier	*ASXL1, EZH2* and *KMT2A*	Deregulation of chromatin modification and impairment of methyltransferases function
Cohesin complex	*STAG1, STAG2, RAD21, SMC1A, SMC3,*	Impairment of accurate chromosome segregation and transcriptional regulation
Splicing factors	*SRSF2, SF3B1, U2AF1, ZRSR2*	Deregulated RNA processing and aberrant splicing patterns

AML patients are risk-stratified at diagnosis based on their genetic background. The 2017 European LeukemiaNet (ELN) recommendation for risk-stratification of AML classified AML genetic mutations into favorable, intermediate, and adverse (Table 3)[12].

Table 3. ELN 17 AML classification (adapted from Hou et al, 2020)

Risk profiles	Subgroups
Favorable	t(8;21)(q22;q22.1); *RUNX1-RUNX1T1*
	inv (16)(p13.1q22) or t(16;16)(p13.1;q22); *CBFB-MYH11*
	Mutated *NPM1* without *FLT3*-ITD
	Mutated *NPM1* with *FLT3*-ITDlow
	Biallelic mutated *CEBPA*
Intermediate	Mutated *NPM1* and *FLT3*-ITDhigh
	Wild-type *NPM1* without *FLT3*-ITD
	Wild-type *NPM1* with *FLT3*-ITDlow
	t(9;11)(p21.3;q23.3); *MLLT3-KMT2A*
	Cytogenetic abnormalities not classified
Adverse	t(6;9)(p23;q34.1); *DEK-NUP214*
	t(v;11q23.3); *KMT2A* rearranged
	t(9;22)(q34.1;q11.2); *BCR-ABL1*
	inv (3)(q21.3q26.2) or t(3;3)(q21.3;q26.2); *GATA2,MECOM(EVI1)*
	Complex karyotype, monosomal karyotype
	-5 or del(5q); –7; –17/abn(17p)
	Wild-type *NPM1* and *FLT3*-ITDhigh
	Mutated *RUNX1*
	Mutated *ASXL1*
	Mutated *TP53*

Chromosomal aberrations are detected in about 50% of adult AML patients. Some of them are transcription factor fusions. The most common transcription factor fusions are PML-RARA, RUNX1-RUNXIT1, MUH11-CBFB and PICALM-MLLT10. These changes belong to the group with favorable cytogenetic risk, which respond well to chemotherapy treatment.

Mutation of the nucleolar protein nucleophosmin 1 (NPM1) gene represent the most frequent recurrent genetic alteration in AMLs, occurring in 25-35% of AML patients[13,14]. NPM1 mutations cause aberrant localization of this protein in the cytosol, instead of the nucleus. The gene product is involved in different cellular processes, including DNA repair, apoptosis, and ribosome biogenesis. These mutations usually occur late in the disease development, and their effect is highly dependent on co-occurring mutations[15].

Fms-like Tyrosine Kinase (FLT3) is the second most commonly mutated gene in AML (25% of AML patients). The mutation activates the tyrosine kinase constitutively, leads to increased blast proliferation, and correlates with poor outcome[16].

Mutations in genes involved in DNA methylation (DNA Methyltransferase 3A (DNMT3a), Ten-Eleven Translocation 2 (TET2), Isocitrate Dehydrogenase (IDH)), and chromatin modifiers (Additional Sex comb-like 1 (ASXL1)) occur early in leukemia progression and have poor prognosis[10,17].

Mutations in Cohesin occur in 10% of AML patients and, in most cases, co-occur with NPM1, DNMT3A, TET2, or RUNX1. Cohesin regulates the separation of sister chromatids, DNA replication, and repair of the damaged double-strand DNA during cell cycle progression. Cohesin mutations most frequently lead to loss of these functions, therefore causing impairment of hematopoietic differentiation[18].

Mutations in RNA splicing factors are most frequently found in secondary AMLs developing from MDS and are linked to poor outcome[19].

Runt-related transcription factor (RUNX1) and CCAAT Enhancer binding protein α (CEBPA) are transcription factors involved in the establishment of definitive hematopoiesis. RUNX1 is associated with gene fusions and other chromosomal rearrangements[20]. It has a favorable prognosis when related to gene fusions. RUNX1 mutation alone, instead, is associated with poor survival[21, 22]. Bi-allelic CEPBA mutations have favorable outcome[23].

Tumor suppressor TP53 mutations are related to complex karyotype, drug resistance, and poor survival[24].

Different types of mutations occur at different times of leukemia progression. Mutations in “landscaping” genes, like genes involved in global chromatin changes such as DNA methylation, histone modification, and chromatin looping, occur early in the evolution of AML, at the pre-leukemic stage, whereas mutations in "proliferative" genes occur later, during leukemia development[17]. Certain mutations, like transcription-factor fusions are thought to be responsible for leukemia initiation. Other common mutations, like DNMT3A, NPM1, CEPBA, IDH1/2, and RUNX1 are usually mutually exclusive with transcription-factor fusions, suggesting that these might have a role in disease initiation. Mutations of genes encoding cohesins, proteins of the spliceosome, signaling proteins, and histone-modifying proteins, are also found to be mutually exclusive, suggesting that one mutation in these pathways is generally adequate for AML pathogenesis[25].

1.3 AML therapy

Despite recent advances in AML treatment, anthracycline-based chemotherapy remains the principal option for treatment. For adult AML patients standard induction therapy consists of 7+3 regimen (7 days of continuous infusion cytarabine (100-200 mg/m^2) and 3 days of intravenous administration of anthracycline (daunorubicin at least 60 mg/m^2 or idarubicin 12 mg/m^2, or mitoxantrone 12 mg/m^2)[26]. Induction therapy can be modified based on estimated genetic risk[27]. In patients with intermediate risk, with FLT3 mutations or CD33 expression, midostaurin or gemtuzumab ozogamicin (GO) can be added to the standard regimen. Moreover, in younger patients with intermediate risk, high-dose cytarabine with anthracycline is recommended as frontline therapy[27]. Instead, in older

patients with adverse risk, hypomethylating agents can be added to induction therapy, or coupled with venetoclax[27].

Around 60-80% of younger patients (< 60 years) respond to induction therapy, while 20% do not. The response is defined as complete remission (CR) if blast count in the BM is below 5% and neutrophil and platelet counts are>1,000/μl and >100,000/μl, respectively[28]. Among older individuals, the percentage of patients who respond is lower, accounting for 40-60%, meaning that every second patient is resistant to induction therapy. In patients with poor or intermediate response, reinduction therapy, which represents the second round of induction therapy, is the therapy of choice [27].

Induction therapy is followed by consolidation therapy, which depends on age and genetic risk group (favorable, intermediate, or adverse)[28]. For patients, younger than 60 years and at favorable risk, recommended treatment is 2-4 cycles of idarubicin with cytarabine (IDAC regimen). In case of intermediate risk, patients can either undergo 2-4 cycles of IDAC, allogeneic hematopoietic cell transplantation (HCT), or high-dose therapy coupled with autologous HCT. In patients older than 60 years with favorable risk, 2-3 cycles of IDAC are recommended, while in those with intermediate/adverse risk no specific consolidation therapy is recommended. Regardless/Nonetheless, 40–60% of AML patients will relapse, due to the emergence of cellular resistance to anti-leukemic drugs[11]. There is no specific therapy of choice for patients with relapse. However, several regimens are used in clinical practice: IDAC, or addition of fludarabine and G-CSF for modified IDAC (FLAG-IDA), or combination of mitoxantrone, etoposide, and cytarabine (MEC), and last, allogeneic HCT[26]. The success rate of these therapies is not particularly high. Thus, there is a compelling need to identify novel strategies to reverse drug resistance.

1.4 Intratumor heterogeneity

Emerging evidence suggests that drug resistance in cancer cells, including AMLs, is a consequence of intratumor heterogeneity (ITH)[28,29]. ITH refers to the coexistence of multiple cellular clones within the same tumor with different genetic, functional, morphological, and molecular features.

Three models have been proposed to explain the occurrence of ITH in cancer: the clonal evolution (CE), the cancer stem cell (CSC), and the plasticity model (Fig. 4)[30,31,32]. The CE model suggests that, initially, all cancer cells are similar to each other, but, due to internal (genomic instability) and external microenvironmental pressures (tumor microenvironment, metabolic changes, chemical influence/chemotherapy), they then acquire genetic and epigenetic modifications, thus giving rise to cellular clones with distinct

properties. The CSC model instead suggests the existence of specific cell populations with the ability to self-renew and differentiate, the so-called cancer stem cells. This model suggests that ITH is a consequence of the differentiation of individual CSCs. The plasticity model represents a bridge between the two models, suggesting the existence of a specific population of cells that creates ITH, the CSCs, but at the same time postulating that any other tumor cell can undergo genetic and epigenetic changes leading to further diversification of the tumor. Furthermore, this model also suggests that tumor cells can dedifferentiate and switch to CSC state.

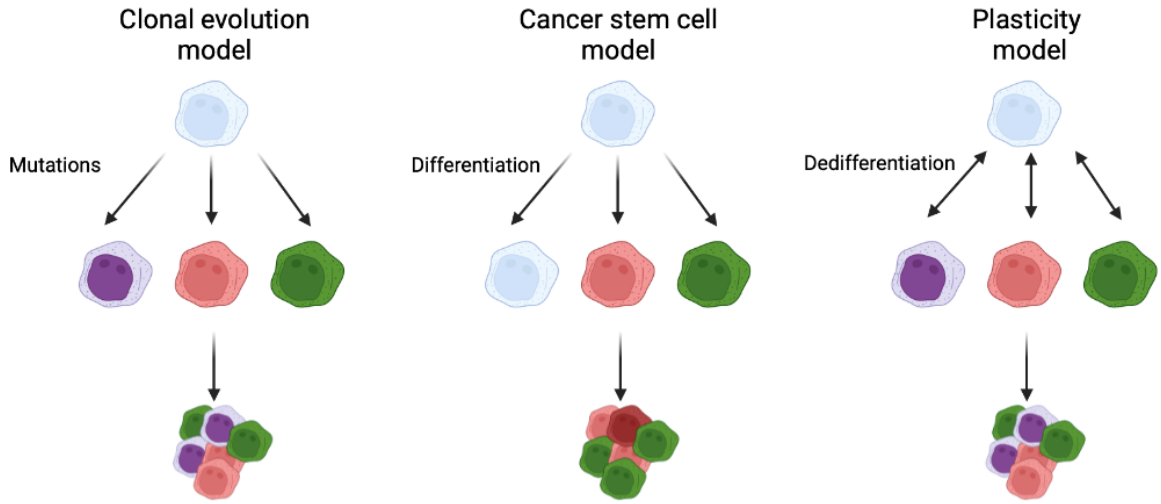

Figure 4. Models of intratumor heterogeneity

CSC is represented in blue, while differentiated cells are shown in other colors. In CE and CSC model arrows are single-directional, suggesting that once differentiation occurs, it can't be reversed. Instead, arrows in the plasticity model are bi-directional, suggesting the possibility of dedifferentiation.

Two main levels of intratumor heterogeneity are generally recognized: genetic and phenotypic. Intratumor genetic heterogeneity is defined by the presence of multiple cellular sub-clones with different genotypes and is the consequence of the progressive accumulation of mutations during leukemogenesis. AML is among cancers with the fewest mutations, with the rare occurrence of genomic instability[25]. Previous studies identified clones with preleukemic HSC mutations, which, upon acquisition of additional mutations, evolve to leukemic clones[17,33,34]. Some mutations are found to be commonly present in patients with leukemia, such are NPM1, FLT3, CEBPA, DNMT3A, IDH1, and IDH2, and the more recently found EZH2, U2AF1, SMC1A, and SMC3[25]. Mutations involved in epigenetic regulation are found to occur early in the development of leukemia, and they are most commonly founder events. Such mutations include DNMT3A, ASXL1, TET2, IDH1, and IDH2[32,34]. Instead, mutations like NPM, FLT3, and RAS appear later in leukemia

development and represent cooperating events. Clonal heterogeneity in AML is a dynamic process with continuous acquisition and loss of different mutations, which together create a complex clonal organization of the tumor[35]. AML genomic clones which acquire the same mutations result in similar phenotypic features, while those that acquire different mutations result in distinct phenotypic profiles[36]. Under environmental pressure, such as chemotherapy treatment, two major types of response are observed: a) the founding clone in the primary tumor may gain mutations and evolve into the relapse clone, or b) a subclone of the founding clone may survive initial therapy, gain additional mutations, and expand at relapse. In both cases, the founder clone is not eradicated by chemotherapy[37]. However, intra-tumoral genetic heterogeneity is not sufficient, per se, to explain the numbers and diversity of tumor clones. Thus, phenotypic heterogeneity appeared as a potential candidate to explain the exceeding high intratumor heterogeneity.

Intratumor phenotypic heterogeneity (also referred to as non-genetic heterogeneity) instead represents specific transcriptional, translational or metabolic traits acquired as a consequence of the phenotypic adaptation of individual cells to the changing tumor microenvironment and the exposure to external stressors, including therapies or the harsh microenvironment, or specific metabolic requirements of cancer cells, as those induced by oncogene expression and hyper-proliferation[38]. Such adaptations are critical for tumor development/maintenance and might contribute to resistance to therapy, independently of (or in addition to) the acquisition of novel mutations.

Initially, phenotypic diversity was described by the existence of blasts with different cellular markers, such as CD34+CD38- cells, which were defined as leukemia stem cells (LSCs)[39]. However, this strategy was abandoned, considering that cells with the same surface markers can still exhibit different behavior[40]. More recent studies applied label-free proteomics to define the set of LSC-specific plasma membrane proteins[41]. With the development of new technologies, other strategies for the identification of different phenotypic clones have emerged. For example, PhenoGraph distinguished different leukemic subpopulations by investigating signaling pathways in normal BM and discovered that expressed pathways coincide with surface markers, while this correlation is lost in AMLs[40]. Deviating gene Expression Profiling Tumor Heterogeneity (DEPTH) algorithm was designed to use gene expression deviation in different cancer types to predict the behavior of different cell populations. Populations with high DEPTH scores had a prevalent association with the common features of high-ITH tumors, e.g., genomic instability, tumor advancement, unfavorable prognosis, immunosuppression, and drug resistance[42].

DNA molecular barcoding enabled tracking of independent cellular clones and revealed the high complexity of tumors[43]. Van Galen et al. combined single-cell RNA

sequencing (scRNAseq) with genotyping to bring together genetic and phenotypic heterogeneity and create an atlas of AML cell states, regulators, and markers that can be used for precision medicine and immune therapies, and demonstrated that cell type compositions correlated with prototypic genetic lesions[44]. Finally, the TARGET-seq tool allows for similar analyses combining mutation detection with whole-transcriptome profiling[45]. As analyses of clonal relationships between phenotypic states have led to conflicting conclusions, the mechanistic relationship between genetic and phenotypic heterogeneities remains unclear.

Among different types of intratumoral phenotypic heterogeneity (transcriptional, epigenetic, metabolic), two phenotypic features were investigated by multiple studies, and they seem to have a great influence other than the development and maintenance of ITH, which are stemness and quiescence.

1.5 Leukemia stem cells (LSCs)

A further level of phenotypic heterogeneity is represented by the presence, within tumors, of rare cancer cells with the unique property of propagating tumors in model systems, so-called tumor-initiating cells (TICs) in solid tumors, or leukemia-initiating cells (LICs) in leukemia[39]. The LIC concept is derived from the observation that only a subpopulation of AML cells with an immature immunophenotype (CD34+, CD38−) can reconstitute leukemia in engraftment experiments using NOD/SCID mice[39,46]. These cells represent a rare and poorly characterized population of cells with stem cell features, such as self-renewal capacity, quiescence, and drug resistance, and are thought to be responsible for the maintenance of the disease as well as for relapse, as a result of their resistance to traditional therapies[47,48]. LICs represent the experimental equivalent of LSCs. LICs are capable of initiating tumor in transplantation assays in experimental models. However, it is still unclear if these cells are responsible for tumor initiation and maintenance in patients.

Despite multiple studies that tried to define the LSC immunophenotype, exact surface markers and phenotype of LSCs are still unknown[49,50]. For example, while hematopoietic stem cells (HSCs) have been demonstrated to switch from quiescent to proliferating state (dormant/active HSCs) and *vice versa*, it is still unknown if LSCs possess the same properties[51,52]. Studies done on quiescent HSCs suggest that after a certain number of divisions, HSCs exhaust and lose their power to regenerate[53]. It is still unknown if LSCs have limited regenerative potential or not. Finally, the BM niche has been shown to support HSC survival and development, while AML cells have been shown to produce factors that

contribute to the remodeling of the BM niche. The full range of AML influence on BM niche, and influence of niche on AML development and survival is still under investigation[54].

1.6 Leukemia cell quiescence

Leukemia cell quiescence is a further level of phenotypic heterogeneity and a putative mechanism of drug resistance, due to the intrinsic resistance of non-proliferating cells to chemotherapy. Quiescence is defined as the cell exit from the cycle (characterized by the four phases G0/G1, S, G2, and M). It is an intrinsic property of normal adult hematopoietic stem cells (HSCs) and is required to maintain an intact self-renewal potential during the life span[55]. In AMLs, a large fraction of blasts within individual samples is not actively cycling and remains in a non-dividing state (from ~70% to ~90%; [56]). The high frequency of quiescent AML blasts has also been demonstrated by *in vivo thymidine incorporation* studies[57]. Quiescent stem cells were shown to evade immunosurveillance as long as they stay in a quiescent state and once they started proliferating, they would be recognized by the immune system and destroyed[58]. These cells showed limited sensitivity to conventional cell cycle-active chemotherapeutic drugs, and they could repopulate tumors after treatments[59,60]. Another study showed that quiescence in pre-LSCs is essential for self-renewal, clonal expansion, and therapeutic resistance[61]. Quiescence in AML might thus play a role in the protection and regeneration of LSCs by the maintenance of self-renewal and limiting DNA damage. In stress conditions, cell cycle arrest is induced to prevent further DNA damage and provide enough time for the tumor cell to recover and induce DNA repair[62]. This finding might be relevant for future therapies, which might affect the survival of leukemia cells by inhibition of cell cycle arrest-induced DNA repair. However, the biological significance of leukemia cell quiescence, underlying molecular mechanisms, and its contribution to the emergence of resistance in AMLs are currently unknown.

1.7 Chemoresistance and relapse

Mechanisms of chemoresistance in Acute Myeloid leukemia are not yet fully understood. Though a few detailed studies are available using patient samples, some studies provide insights into possible causes and mechanisms of chemoresistance.

For decades, chemoresistance was known to be the consequence of genetic alterations which give an advantage to some leukemic cells, so they can survive chemotherapy and eventually relapse[11,63,64]. Consistently, it was shown that relapse samples contain new mutations, as compared to the primary ones, suggesting that chemotherapy leads

to the appearance of new mutations[37]. Shlush et al. provided an opposite view, suggesting that chemotherapy doesn't influence mutagenesis, but only selects cells that carry pre-existing mutations[28].

There is increasing evidence that non-genetic processes drive drug tolerance, presenting a major hurdle to successful cancer therapy. Drug-tolerant persistent cells, e.g. cells that persist at the end of treatment, are emerging key players of drug resistance and are identified across a wide range of tumors in response to chemotherapy and targeted agents[65,66,67].

Recently, epigenetic/phenotypic changes were recognized over genetic changes as the main cause of survival of leukemic cells after treatment and subsequent relapse. Epigenetic changes comprise all non-genetic changes, including epigenetic modifications (e.g., DNA-methylation), transcriptional and translational modifications, as well as extracellular modifications (niche signaling, chemotherapy, etc.).

Figueroa et al. discovered that AMLs have a common aberrant DNA-methylation signature consisting of 45 genes, mostly hypermethylated. These genes are likely to be part of a common epigenetic pathway that is involved in the leukemic transformation of hematopoietic cells[68]. Landau et al. suggested a model in which gene-methylation patterns coincide with novel somatic mutations to propagate new genotypes in the progeny populations[69]. Li et al. explored the influence of epigenetic modifications on disease progression and relapse. They observed variable epiallele modifications during disease progression. Opposite to previous studies, they discovered that epiallele diversity doesn't always follow changes in somatic mutations and suggested a model in which the disease follows two different kinetics, genetic and epigenetic, which mostly follow independent kinetics. Moreover, they noticed that shifts in epiallele frequency occur at early time points of disease progression, while increased somatic mutations were observed at later time points, suggesting that epigenetic modifications anticipate genetic modifications during disease progression[70].

Furthermore, phenotypic states, like stemness and quiescence can also influence disease progression or relapse. Stemness is a biological property defined by an immature phenotype similar to that found in normal stem cells. LSCs, as expected, possess an immature phenotype, though also other, more mature cells, can express more primitive traits. As above mentioned, Slush et al. showed that relapse can be caused by both LSCs and lineage-committed cells, though in both cases relapse is due to cells with stem cell properties[34].

Many studies explored the role of LSCs on survival and relapse. Ho et al. demonstrated 9-90-fold increased frequency of LSCs in the relapse samples, though the same

study raised the issue of the correct detection of LSCs, considering the paucity of unique markers for LSCs [71]. Instead, Boyd et al. observed that there is no preferential survival of LSCs after treatment and that these cells are equally eliminated as more mature progenitors are, leaving open the question of the cell type responsible for relapse[72]. Another study identified a list of 17 genes (LSC17) preferentially expressed in populations with high LSC content (CD34, LAPTM4B, ARHGAP22, LOC284422, KIAA0125, MMRN1, DNMT3B, SOCS2, CDK6, NGFRAP1, CPXM1, ZBTB46, DPYSL3, NYNRIN, GPR56, AKR1C3, EMP1) and demonstrated that their expression is a good predictor of disease relapse, lower response rates to standard induction chemotherapy, shorter survival and higher rates of chromosome aberrations[73]. Van Galen et al. demonstrated that tumors consist of multiple cell populations (HSC-like, progenitor-like, GMP-like, promonocyte-like, monocyte-like, or cDC-like malignant cells), and that cell composition is greatly influenced by the genetic background of the tumor. However, this study also confirmed that tumors enriched in HSC/progenitor-like cells have significantly worse outcome[44].

Stemness is commonly related to quiescence, which represents a pause in the cell cycle, and can be found in normal as well as cancer cells. Both stemness and quiescence were suggested to be responsible for leukemia cell survival and relapse[74,75]. In most cases, this is explained by the mechanism of action of the chemotherapy drugs, which mostly act on dividing cells. The quiescent state of cells would protect them from these chemotherapeutical agents, thus supporting their survival and favoring relapse[76]. Wang et al. investigated the influence of quiescence on disease outcome and chemotherapy resistance. They showed that patients with a higher percentage of quiescent cells are predicted with worse outcome. Moreover, they demonstrated preferential survival of quiescent cells after chemotherapy, suggesting that quiescence might be a protective mechanism against chemotherapy[77]. Yilmaz et al. demonstrated the importance of long-term quiescence in a relapse in patients, based on patients with very-late relapse (more than 5 years). They showed by WES that in most of these patients relapse was caused by a founder clone, which then evolved into the relapse clone, suggesting that these cells were in a quiescent state for a prolonged time, meanwhile acquiring new mutations which enabled them to relapse[78].

Another important factor for leukemia development, survival, and relapse is the BM niche, which represents the microenvironment in which healthy hematopoietic and malignant AML cells reside. BM stromal cells are among the most important cells for the maintenance of the hematopoietic niche, as well as the major support for the development and differentiation of hematopoietic cells. They also have immunomodulatory effects, by creating an immunosuppressive niche that induces self-tolerance. However, this feature can also create a niche permissive for the development and maintenance of AML[79]. Van Galen

highlighted the importance of the BM niche in AML, which was found to have fewer numbers of T cells and cytotoxic T cells, and increased numbers of regulatory T cells, forming an immunosuppressive environment for leukemia growth. Monocyte-like cells were found to be the most important immunomodulatory cells since they have been found to inhibit T cell activation[44]. Wang et al. described the influence of human mesenchymal cells (hMSC) in leukemia survival by inducing quiescence in leukemic cells, thus protecting AML cells from chemotherapy[77]. Several studies highlighted the importance of endosteal and vascular niche for AML survival, mostly by induction of quiescence and stimulation of LSC self-renewal and proliferation[54,80,81]. Normal and preleukemic HSCs were found to localize in an endosteal niche, as well as around arterioles and sinusoids[82,83]. In AMLs, blasts create a proinflammatory environment leading to decreased numbers of osteoblasts, inhibition of their differentiation, and decreased numbers of residual normal HSCs, which can't survive in this newly created niched[54]. During leukemia development, remodeling of vascular niche leads to increased numbers of BM vessels. Moreover, endothelial cells support AML cells by inducing proliferation and pro-survival signals[81].

Another study suggested the use of leukemia-associated plasma membrane (PM) proteins to detect leukemia-associated phenotypes, which could be detected in over 90% of patients and could also predict the disease outcome. They showed that PMs can be used to identify genetic clones and also to perform longitudinal tracking of clonal evolution (primary vs relapse)[41].

Current literature provides robust evidence suggesting that relapse originates from rare persistent AML cells which survive chemotherapy (data from both patients and model systems; Fig. 5)[72].

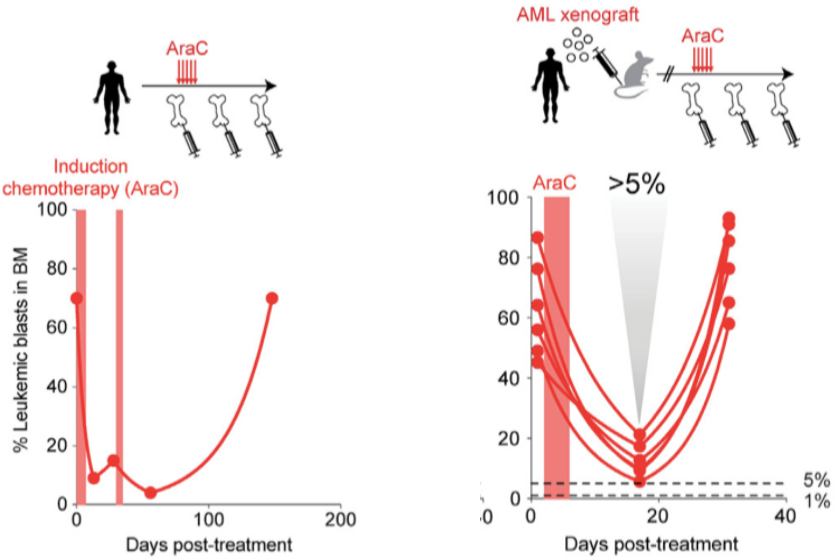

Figure 5. Relapse in patients and model systems (adapted from Boyd et al)

On top of each graph experimental scheme is shown. On the left side, data from a single human sample is shown, while on the right side data from individual AML xenografts are shown. Chemotherapy treatment was a single-drug treatment with cytarabine. Graphs show the influence of chemotherapy treatment on engraftment levels over time, with day 14 post-chemotherapy being the lowest engraftment time point.

An open question is whether persistent cells are drug-resistant or not, and if their survival is, in fact, related to their intrinsic chemoresistant features, related to their quiescence, or to a protective microenvironment. In both patients and models systems, post-chemotherapy there is an evident drop in the percentage of leukemic blasts in BM. In humans, less than 5% of leukemic blasts in BM are considered complete remission. Instead, in model systems, remission represents a significant drop in the percentage of leukemic blasts in BM. Depending on the initial percentage of leukemic blasts, during remission percentages in BM may vary. In both, the patients and model systems, day 14 represents the lowest engraftment time point, after which initial relapse starts.

Clinical data suggest that persistent cells of cases that will relapse are truly drug resistant[17,25]. Patients who don't show an initial response to induction or reinduction chemotherapy or those who relapse after chemotherapy are considered resistant to the next round of chemotherapy[27]. Their therapy is usually switched to alternative treatments, such as allogeneic HCT or personalized medication specific to the mutational pattern of given patients.

Model systems, instead, provided conflicting results, with some suggesting drug resistance, while others sensitivity, even after several rounds of chemotherapy[72,84]. In the latter, the selection of cell cycle-restricted (diapaused) cells was proposed as the mechanism underlying the emergence of drug-sensitive disease. Duy et al[84]., using both human AML samples and PDX models, hypothesized that AML relapse is dependent on the persistence of a subset of resistant cells undergoing a senescence-like resilient state, potentially mimicking a diapause state, to survive genotoxic stress caused by chemotherapy and eventually, reconstitute the disease (Fig. 6). Embryonic diapause is an evolutionarily conserved strategy featured by reversible growth-arrest (up to many months) of blastocysts[85,86], allowing survival during stressful environmental conditions. Diapause, in fact, is defined as a reversible state of suspended embryonic development triggered by unfavorable environmental conditions[87]. It has also been demonstrated that drug-resistant persistent cells share a diapause-like dormancy signature in solid tumors (e.g., colorectal cancer)[88], evidencing an emerging role of this embryonic state in the context of

chemoresistance, which however needs more detailed characterization. The selection of specific drug-resistant genotypes or phenotypes, instead, has not been yet explored.

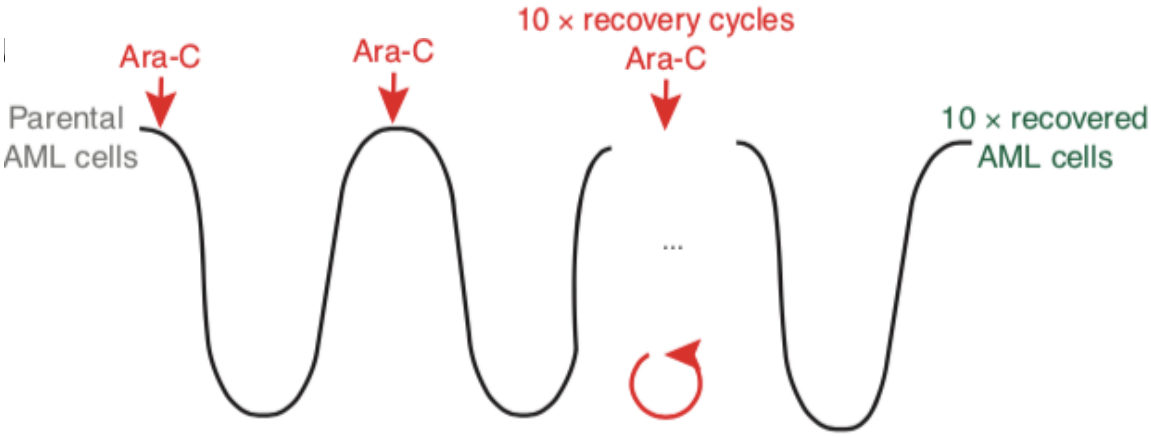

Figure 6. AraC treatment of AML demonstrating sensitivity after multiple rounds of chemotherapy

Human AML cells were treated with 10 cycles of AraC. After each cycle, a number of cells would drop and then start increasing again, and cells were then retreated. Through 10 cycles of AraC sensitivity of AML cells to AraC didn't change (adapted from Duy et al).

2 Hypothesis and Aims of the project

The *working hypothesis* of my project is that chemoresistance in AMLs is associated with specific phenotypic states that characterize rare cell populations within the pool of quiescent leukemic cells. These cells are then selected by chemotherapy and represent the cellular basis of the relapse.

The main goals are: i) to define the transcriptional circuits that feature this intrinsically chemoresistant cell population, its cell cycle properties, and identity-relation with LICs; and ii) to characterize intracellular signaling pathways and (micro)environmental cues that induce cell cycle restriction and specific phenotypic states associated to chemoresistance.

Specific aims are:

1. ***Cellular, transcriptional and functional characteristics of quiescent leukemic cells.***
   Here, I will set up time-course experiments that will take advantage of our label-retaining (LR) system (H2B-GFP) to purify the non-dividing (quiescent) populations of cells. I will use cell cycle tracking assays (BrdU and KI67) to reveal the truly quiescent population of cells. Then, I will use scRNAseq to resolve the phenotypic heterogeneity of proliferating *vs* quiescent leukemia cells. I will define molecular pathways and gene signatures specific to quiescent leukemic cells. Finally, I will perform functional assays to investigate the link between quiescent cells and LIC content found in this population.
2. ***Role of chemotherapy on transcriptional and functional profiles of chemotherapy-persistent leukemic cell populations.***
   I will set up time course experiments in which I will use different chemotherapy regimens to identify the chemoresistant leukemic cell population. I will also use LR assays, as well as cell cycle labeling assays to investigate the relationships between quiescence and chemoresistance. Further on, I will define transcriptional properties of chemoresistant persistent cells and extract pathways and genes specifically enriched in this population, to define gene signatures that can be further targeted. Finally, I will investigate how chemotherapy affects LIC content by the usage of different functional assays.
3. ***Clonal architecture of survivor Leukemic Stem Cells (LSCs).***
   Here, I will take advantage of a lineage tracing approach using cellular barcodes to identify the clonal composition of the residual chemotherapy-persistent cell

population and track it back to the growing leukemia. I will then define pathways and genes specifically enriched in this population, to identify gene signatures that can be further targeted.

4. ***Investigation of niche localization of distinct AML sub-populations.***

   I will focus here on defining the localization of quiescent cells within the BM and understanding if these populations establish a specific niche or not. Moreover, I will explore the influence of chemotherapy on BM localization and compartmentalization.

3 Materials and Methods

3.1 AML patient-derived xenograft (PDX) models

3.1.1 Patient samples

Acute Myeloid Leukemia (AML) samples were collected from patient peripheral blood (PB), bone marrow (BM), or other tissues given their consent. Informed consent was obtained from all enrolled patients in compliance with the principles of the World Medical Association Declaration of Helsinki. Samples were collected from two patients coded as AMLIEO20 and AML9. AMLIEO20 patient was 42 years old female with therapy-related AML post-treatment for breast cancer, while AML9 patient was male with primary leukemia (information about age not available). According to French-American-British (FAB) classification of AML, AMLIEO20 belongs to M4 subtype, or acute myelomonocytic leukemia, while data for AML9 patient were not available. AMLIEO20 patient had 9:11 translocation, with wild-type FLT3 and NPM1, and it was classified as intermediate risk, while AML9 was a complex karyotype, with wild-type FLT3 and NPM1 and classified as adverse risk group.

3.1.2 Generation of AML PDX models

To produce PDX models, human samples, freshly isolated from patients, were transplanted into murine experimental models, NOD SCID IL2 RG null mice, which were chosen as the optimal model based on their ability to support greater engraftment of human hematopoietic stem cells compared to other models. Successful engraftment was observed in 70% of the mice, while the latency was highly variable among different AML PDX models (showing a range from 4 to 8 weeks before the first visible engraftment). PDX models went through 5 passages. Passage 5 cells were used for all the experiments presented in the thesis. Whole exome sequencing analysis showed that in the AML9 PDX model minor clones expanded through passaging changing the initial patient mutational structure, however, the PDX model remained stable through further passaging (Fig. 7a). Patient data were not available for AMLIEO20, however, WES data from the PDX model showed that this model didn’t change through passaging (Fig 7b).

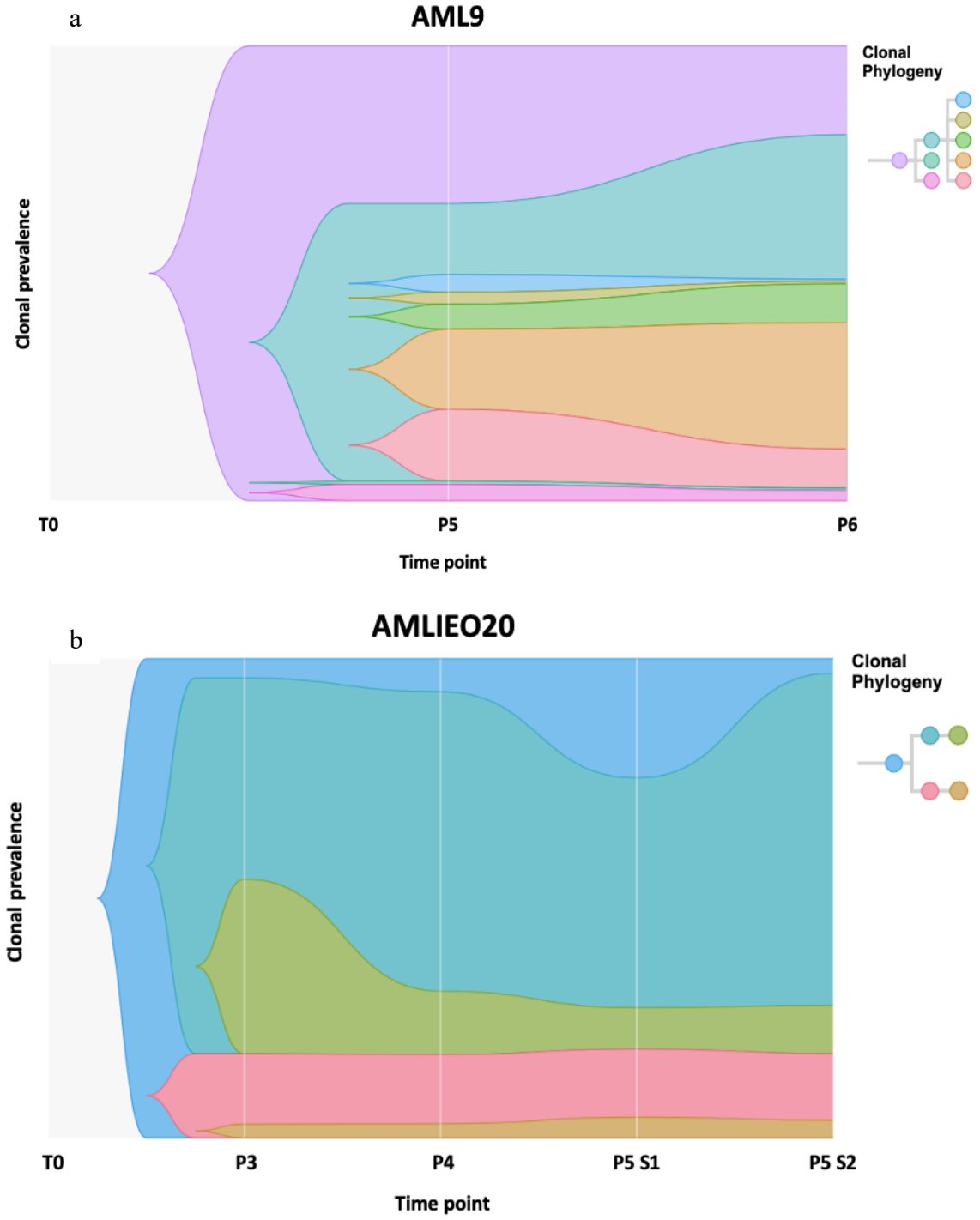

Figure 7. Clonal composition of both PDX models (AML9 and AMLIEO20) remains stable through passaging.

Clonal evolution graphs are shown for AML9 (a) and AMLIEO20 (b). Graphs show clonal prevalence per time point. In AML9, clonal evolution is shown for passage 5 (P5) and passage 6 (P6), while in AMLIEO20, clonal evolution is shown for passage 3 (P3), passage 4 (P4), passage 5 sample 1 (P5 S1) and passage 6 sample 2 (P6 S2). Clonal phylogeny is shown on the right side of each graph (Vlachou, Cheloni, Cammarata et al. manuscript in preparation).

3.2 Animal experimentation

All experiments including animals were conducted by the Italian Law (Legislative Decrees no. 116/92 and no. 26/2014), which enforces the EU Directives (86/609/EEC of 24 November 1986 and 2010/63/EU of 22 September 2010) on the approximation of laws, regulations and administrative provisions of the Member States regarding the protection of animals used for experimental and other scientific purposes. Mice were housed and taken care of accordingly to the guidelines set out in Commission Recommendation 2007/526/EC - June 18, 2007. At the end of the experiments, all mice were euthanized by inhalation of high concentrations of carbon dioxide (CO_2).

3.2.1 AML Transplantation

In my experiments, I used PDX models already established in the group, as previously mentioned (§3.1). In most cases, 10^6 cells were selected as the optimal transplantation cell dose. This cell number was chosen to ensure positive engraftment in animals at optimal experimental timing (4-6weeks, depending on the model). AML cells were resuspended in 250 µl of phosphate-buffered saline (PBS and the mixture was kept on ice until transplantation. NSG mice were heated in their cages using infrared light lamps. Upon lateral tail vein dilatation, mice were transferred into lab animal restrainers, where transplantation *via* lateral tail vein injection was performed. Mice were monitored post-transplantation to ensure their well-being. Most of the animals would experience only mild discomfort during the procedure.

3.2.2 Limiting dilution and serial transplantation assay

Limiting dilution transplantation assays were used for LSC frequency estimation. The general transplantation protocol was used (§3.2.1), however, instead of using a single transplantation dose of 10^6 cells, scalar cell doses of 100, 500, 1,000, and 5,000 cells were used. Cell mixtures were prepared by serial dilution. The final volume for transplantation was 250 µl. Leukemia engraftment was observed 4-6 weeks post-transplantation, depending on the AML model used. All mice were monitored periodically and sacrificed by CO_2 inhalation when they reached 80% engraftment or, in the absence of positive engraftment in PB, at a maximum 6 months post-transplantation. Mice found dead without confirmed leukemia engraftment were excluded from the analysis. LSC frequency calculation was

performed by ELDA (extreme limiting dilution analysis; http://bioinf.wehi.edu.au/software/elda/) software.

3.2.3 Engraftment tracking

Weekly bleedings were performed on transplanted mice to follow engraftment over time. NSG mice were heated by infrared light lamps and then transferred to laboratory animal restrainers. After a superficial cut on the tail, blood (35-140 µl) was collected from the lateral vein of the mice, mixed with the appropriate amount of ethylenediaminetetraacetic acid (EDTA; 0.5M, pH 8.0; 15 µl EDTA for 35 µl of blood, or 60 µl EDTA for 140 µl of blood), used as an anticoagulant, and kept on ice till red blood cell (RBC) lysis. A hypotonic solution (8.125 mg/ml NH_4Cl, 1 mg/ml $KHCO_3$, 0.13 mM EDTA in dH_2O) was used for RBC lysis. In detail, 500 µl of RBC lysis were added to 50 µl of blood/EDTA, and samples were gently mixed by tube inversion and incubated for 10 min at 4 °C. After RBC lysis, cells were labeled with anti-human CD45 antibodies (1:100 dilution in PBS, 1h incubation at 4 °C). Analysis of engraftment was performed by flow cytometry.

3.2.4 Label retaining assay

To perform *in vivo* LR assay, two of our PDX models were infected with a lentivirus containing the histone 2B (H2B) – green fluorescent protein (GFP) vector[89], which allows division tracking based on the inducible (tet-off) expression system. In absence of doxycycline, H2B-GFP is stably expressed in over 99% of the cells. Once doxycycline is added, it suppresses the expression of H2B-GFP, allowing the distinction of leukemic blasts into quiescent (those which have not divided and retain the full GFP signal, assigned as GFP-high) and proliferating (cells that have divided during the chasing period and, as a result, diluted the GFP signal). Cells that have undergone 1-8 divisions during the chasing period still retain a detectable signal (GFP-low). Cells that have divided more than 8 times lose completely the H2B-GFP-specific signal and become GFP-negative (GFPneg) (Fig. 8). Doxycycline is given to the mice *via* modified food pellets at a dose of 625 mg/kg. Chasing started upon visible engraftment (10-30% of human cells) and ended with the end of the experiment.

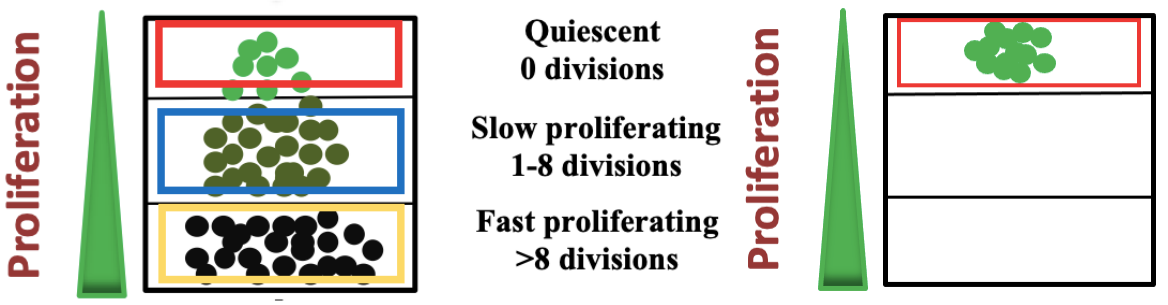

Figure 8. H2B-GFP signal dilution scheme (modified from Vlachou et al. (manuscript in preparation)).

H2B-GFP signal dilution shown after 3 weeks of doxycycline chasing. Population gating is represented by color-coded gates (red- quiescent cells, blue- slow proliferating cells (cells which proliferated 1-8 times in 3 weeks), yellow- fast proliferating cells (cells which proliferated more than 8 times in 3 weeks))(left). Positive control (non-doxycycline treated sample) is shown on the right.

3.2.5 Chemotherapy treatment

Cytarabine (AraC) is a chemotherapeutical used in the treatment of leukemias and lymphomas. It belongs to the group of antimetabolite drugs, and as a pyrimidine analog, it integrates into the DNA, where it causes DNA replication block, specifically in the S phase of the cell cycle, making it a drug used for rapidly proliferating cells[90]. Doxorubicin is part of the anthracycline group of chemotherapeutic agents. Doxorubicin is used to treat multiple cancer types, like soft tissue and bone sarcomas and cancers of the breast, ovary, bladder, and thyroid. It is also used to treat acute lymphoblastic leukemia, acute myeloblastic leukemia, Hodgkin lymphoma, and small cell lung cancer[91]. The most commonly used treatment for induction therapy of AML in clinics is "7+3" combined regimen of cytarabine with anthracycline, where AraC is given for 7 days, while anthracycline is given for the first three days of treatment, overlapping with AraC[26,27]. In murine models, AraC is used either as a single agent for 5 days[72] or a modified "5+3" combined regimen of AraC and anthracycline is given[92]. Both these two chemotherapy regimens were used in the present study. Single treatment, with AraC only, was given for 5 consecutive days at 100 mg/kg intraperitoneally (IP). Combined treatment included AraC (50 mg/kg for 5 consecutive days IP) and doxorubicin (1.2 mg/kg for three consecutive days IP) with both drugs administered in the first three days of treatment and then AraC alone for the last 2 days. In initial experiments, we administered doxorubicin IP and no substantial toxicity was observed. During chemotherapy, mice were monitored and their body mass was followed, in case of worsening of their overall condition or loss of body weight over 20%, mice were sacrificed.

3.2.6 *In vivo* bromodeoxyuridine (BrdU) incorporation

BrdU incorporates newly synthesized DNA, enabling the identification of actively proliferating cells. For the *in vivo* BrdU assay, NSG mice were injected with 1 mg of BrdU (stock solution: 10 mg/ml in sterile PBS, BD). Injections were given intraperitoneally (IP), twice, at a 6-hour interval. Mice were sacrificed 6 hours after the last injection (12 hours BrdU pulse). Tissues (BM and SPL) were collected and labeled with anti-BrdU and other antibodies. BrdU incorporation was then assessed by flow cytometry.

3.2.7 Tissue processing for cell collection

After BM and SPL collection, any remaining fibrous tissue and muscle were removed mechanically from the surface of the bones, and both tissues were mechanically processed, and filtered through a 70 μm cell strainer. Cells were then, either frozen (in freezing media, consisting of 90% South American fetal bovine serum (SA-FBS, Euroclone) and 10% dimethyl sulfoxide (DMSO, Sigma-Aldrich) in a cryobox at – 80 ºC) or purified by Ficoll-Paque Plus (GE Healthcare Cytiva Life sciences; 1:1 ratio between Ficoll and sample, centrifugation at 300 x g, 35 min, 16 °C, deceleration off). After centrifugation, the cell ring was collected, and cells were washed with PBS and further used for other procedures.

3.3 Flow cytometry analysis and fluorescence-activated cell sorting

Flow cytometry was used for engraftment and cell cycle analyses. The acquisition was performed on BD FACSCelesta™ instruments. Sorting was performed using BD FACSAria™ and BD FACSMelody™ instruments to isolate specific leukemic populations. Sorting was based on the signal of H2B- GFP reporter (GFP-high, -low, -negative) or blue fluorescent protein (BFP) signal (reporter in cells infected with high complexity libraries of expressed barcodes). Cells were resuspended in presorting media (PBS containing 2% SA-FBS, 2% penicillin/streptomycin (pen/strep) and 2 mM EDTA) at a concentration of 5 x 10^6 per ml. Sorted cells were collected in post-sorting media (RPMI containing 33% North-American FBS (NA-FBS)). Analysis was performed using the FlowJo™ software (BD; version 10.5.2 or higher).

3.3.1 Engraftment analysis

To determine the presence and relative representation of human leukemia cells in the murine PB, BM, and SPL, cells were labeled with anti-human CD45 antibodies. In detail, 10^6 cells were resuspended in 50 µl of antibody/PBS mix (antibody dilution 1:100) and incubated for 1 hour at 4 °C. Post incubation, cells were washed, fixed in 4% paraformaldehyde (PFA), and acquired by flow cytometry.

3.3.2 Cell cycle analysis

To determine the cell cycle status, available assays, exploiting incorporated BrdU and intracellular KI67 antigen expression were used, coupled with a label for total DNA content, which in the present experiments was DAPI.

3.3.2.1 BrdU incorporation analysis

To fluorescently label DNA incorporated BrdU, the BD APC BrdU flow kit was used. Murine tissues (BM and SPL) were collected and harvested, and 10^7 BrdU pulsed leukemic blasts were used. Cells were optionally stained for cell surface antigens and then fixed and permeabilized with BD Cytofix/CytopermTM and CytopermTM Permeabilization Plus buffers. In detail, cells were resuspended in 100 µl of Cytofix/CytopermTM buffer and incubated for 30 min on ice. Cells were then resuspended in 100 µl of CytopermTM Permeabilization Plus buffer and resuspended for an additional 10 min on ice. After an additional fixation step with BD Cytofix/CytopermTM, cells were treated with DNase (diluted to 300 µg/ml in PBS) for 1 hour at 37°C to expose the incorporated BrdU. The cells were stained with an anti-BrdU antibody (APC BrdU Flow kit, BD; diluted 1:50 in 1X Perm/Wash buffer) along with any other intracellular antigen of choice, and left incubating for 1 hour on ice. After each step, cells were washed with 1ml of 1X BD Perm/Wash Buffer. Finally, the cells were stained for total DNA levels with DAPI and kept at 4°C until FACS analysis.

3.3.2.2 KI67 analysis

KI67 antigen expression is related to cell proliferation. KI67 is found to be expressed in all phases of the cell cycle except G0, making it this way, a specific negative marker for quiescent cells[93]. Murine tissues (BM and SPL) were collected and harvested, and 10^7 leukemic blasts were used. Cells were optionally stained for cell surface antigens and then fixed and permeabilized with BD Cytofix/CytopermTM and CytopermTM Permeabilization

Plus buffers. In detail, cells were resuspended in 100 µl of Cytofix/CytopermTM buffer and incubated for 30 min on ice. Cells were then resuspended in 100 µl of CytopermTM Permeabilization Plus buffer and resuspended for an additional 10 min on ice. After an additional fixation step with BD Cytofix/CytopermTM, cells were stained with an anti- KI67 antibody (PE-Cy7 conjugated, clone B56, BD) diluted 1:50 in 1X Perm/Wash buffer (BD Perm/WashTM buffer 10X diluted in dH2O) and incubated 1 hour on ice. After each step, cells were washed with 1ml of 1X BD Perm/Wash Buffer. Finally, the cells were stained for total DNA levels with DAPI and kept at 4°C until FACS analysis.

3.3.2.3 DNA content analysis

DAPI was used for labeling total DNA content. DAPI is a fluorescent dye, which has the ability to bind to adenine-thymidine-rich regions of DNA, and in this way fluorescently label total nuclear DNA[94]. In the experiments discussed in the present study, after BrdU/KI67 staining, cells were stained with DAPI and kept at 4°C until FACS analysis.

3.3.3 Proliferation analysis

FlowJo proliferation platform was used to model divisions based on fluorescence decay due to doxycycline chasing in H2B-GFP AML models. Analysis was performed by selecting the undivided population (doxycycline non-treated control) of cells first and then applying the same selection to the samples which were chased with doxycycline. The fixed ratio was set at 0.5, considering that with each division cells should lose half of their fluorescent signal, and peak coefficient of variation (peak CV) around 4-5%. Model fitness was assessed visually by the mean root mean square (mRMS) value, which is a measure of the distance of the composite model line from the histogram of the data, and it should be kept at the lowest value possible. Data were further described by the following statistics:

Percentage divided: the percentage of original cells that have divided.

Division index: the average number of cell divisions that a cell in the original population has undergone (including the undivided cells).

Proliferation index: the average number of divisions that a dividing cell in the original population has undergone.

Expansion index: the number of cells found in the sample which originate from a cell from the starting population

Replication index: the number of cells found in the sample which originate from a cell from the starting population which went into division

3.4 Imaging

3.4.1 Sample preparation for imaging

3.4.1.1 BM preparation for sectioning

After collection from the mice, BM was fixed in 4% paraformaldehyde (PFA) overnight. The next day, BM samples were washed in PBS and then transferred to 10% EDTA for decalcification at 4 °C for 1 week. EDTA was changed every 2-3 days. After decalcification, samples were washed in PBS, embedded in low-melting agarose (NuSieve®GTG®Agarose, Lonza), and left in the scaffold until agarose became solid[95].

3.4.1.2 SPL preparation for sectioning

After collection from the mice, SPL was fixed in 4% PFA overnight. The next day, SPL samples were washed in PBS, and then embedded in low-melting agarose and left in the scaffold until agarose became solid (§3.4.4.1).

3.4.1.3 Vibratome sectioning

Vibratome sectioning was used for cutting slices with the appropriate thickness for confocal microscopy, with which samples can be visualized along the z-axis, enabling in-depth analysis of the sample. Slices were cut approximately 150 μm thick and then stained with Hoechst 1:2,000 in PBS overnight at 4 °C. The next day, slices were washed 3 times with PBS and mounted on glass slides for acquisition at the confocal microscope.

3.4.2 Microscopy settings

Images were acquired by confocal microscope (Leica SP8 AOBS confocal laser scanning microscope). Objectives 10x/0.30 HC PL FLUOTAR and 20x/0.75 HC PL APO

IMM CORR CS2 we used to acquire images at 512 x512 resolution, with pinhole size 1.27. For GFP and Hoechst signal acquisition, 405 nm Diode and Argon (488 nm) excitation lasers were used. LAS X software was used for image acquisition, processing, and quantification. Image analysis was performed with ImageJ software (NIH; version 1.52s or higher).

3.5 IC50 assay *in vitro* for chemotherapy drugs

To perform *in vitro* experiments on H2B-GFP AML PDX models, cells were cultured in RPMI-based media supplemented with 20% North-American FBS (FBS, NA), 1% of 5637 (bladder carcinoma cell line)-conditioned medium (5637 CM), and 2% pen/strep, and incubated in 37 °C 5% CO2 incubators.

The half maximal inhibitory concentration (IC50) assay is an *in vitro* assay that calculates the concentration of a drug needed to cause 50% inhibition of a certain biological function or component. The IC50 assay was used in the present study to compare the effect of chemotherapy drugs (AraC and doxorubicin as single agents) on previously chemotherapy treated *versus* previously nontreated cells. A linearity test and growth curve analysis were performed prior to the IC50 assay to select optimal cell concentration.

3.5.1 Linearity test

A linearity test was performed to check which cell concentrations cells still followed linear growth. For this purpose, cells were plated in decreasing concentrations (from 500,000 to 0, diluting 1:2, in triplicates) in 50 µl of media. Cell luminescence was recorded every 24 hours, starting at 0 hours and ending at 72 hours. CellTiter-Glo ® Luminescent Cell Viability Assay kit (Promega) was used to determine cell luminescence. This method allows the estimation of cell numbers based on the luminescence they emit. CellTiter-Glo reagent (50 µl) was added to cells immediately before the acquisition, and cell luminescence was then recorded by GloMax® Plate Reader (Promega).

3.5.2 Growth curve

A growth curve analysis was conducted to follow the doubling time of cells. Concentrations between 1,000 and 10,000 cells in 50 µl of media were used. Cell luminescence was recorded every 24 hours, starting at 0 hours and ending at 72 hours.

CellTiter-Glo reagent (50 µl) was added to cells immediately before the acquisition, and cell luminescence was then recorded by GloMax®.

3.5.3 IC50 assay

Based on the linearity and growth curve tests, 4,000 cells in 50 µl of media were determined as the optimal cell concentration for the IC50 assay. For both AraC and doxorubicin IC50 assays, 4,000 cells were plated per well (96-well plate) in 50 µl of media, in triplicates. Cells were left to rest for 24 hours. Starting chemotherapy dose was either stock concentration or 10mM dose, which was selected based on previous experience in the lab. For AraC, serial 1:10 dilution was performed starting from a 10mM stock solution until a final concentration of 0.001 nM, while for doxorubicin serial 1:5 dilution started from a 3.67 mM stock concentration up to a final concentration of 0.37 nM. An intermediate 1:100 dilution was prepared for both drugs before the addition to the cells. Cell luminescence was recorded every 24 hours, starting at 0 hours and ending at 72 hours. CellTiter-Glo reagent (50 µl) was added to cells immediately before the acquisition, and cell luminescence was then recorded by GloMax®. IC50 calculation was performed using GraphPad Prism software (version 9.2.0).

3.6 *In vivo* clonal tracking

Clonal tracking represents the tracking of the progeny of a single cell. Different barcode libraries have been developed to follow individual cells and their progeny. The idea of using molecular identifiers for clonal tracking was first established in the context of genetic analyses: endogenous (*e.g.* mutations) or exogenous (*e.g.* short barcoding sequences inserted in the human genome through retroviral or lentiviral transduction) elements would allow the identification of clones with a common cellular origin that could be followed by DNA sequencing. Novel types of clonal tracking approaches have been developed and, for the present study, the 3rd generation lentiviral Perturb-seq Guide Barcodes (GBC) library (Addgene #85968)[96,97] was used. The GBC library contains approximately10 x 10^6 unique barcode sequences (18-nucleotide long), which can be expressed and followed by single-cell RNA sequencing, as well as puromycin resistance (PuroR) selection marker and the BFP fluorescence reporter. The experimental strategy consists in stably integrating unique Perturb-seq vector GBC barcodes in individual LSCs, whose progeny can then be followed by GBC barcode expression.

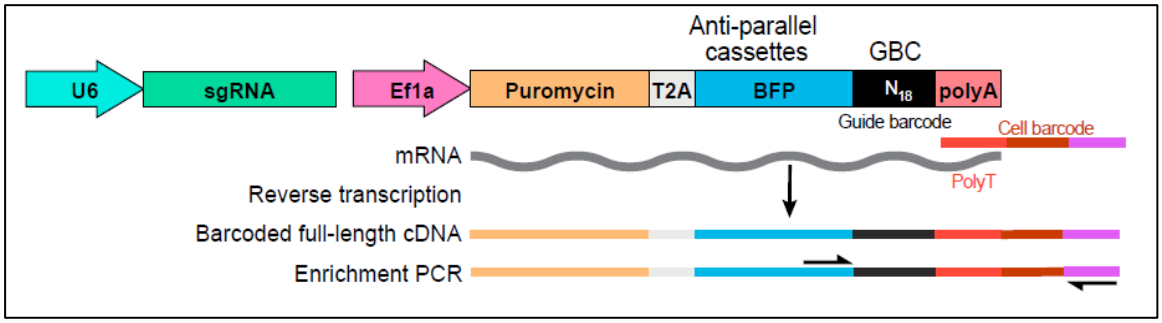

Figure 9. Perturb-seq Guide Barcodes (GBC) library vector structure.
3rd generation lentiviral vector contains a random 18-nt GBC between the blue fluorescent protein (BFP) and polyadenylation signal sequences. The vector contains genes that encode for puromycin and ampicillin resistance and the reporter gene TagBFP. Puromycin resistance and TagBFP are constitutively expressed under the control of the EF1α promoter.

3.6.1 Lentivirus production- Packaging cell line and plasmids

The cell line of choice for viral transfection was HEK293T, also known as the 293 T cell line, derived from the human primary embryonic kidney 293 cell line. 293T cells are commonly used for lentiviral production due to their high transfection efficiency. 293T cells were cultured in DMEM (Lonza) supplemented with 10% FBS, SA (Microgem), 2 mM L-Glutamine (Lonza), 100 U/ml penicillin, and 100 U/ml streptomycin (Pen/Strep stock, Lonza).

To produce 3rd generation lentiviral particles, the following plasmids were used:

- pMD2.G VSV.G (Addgene #12259): encoding the G protein of vesicular stomatitis virus (VSV-G)
- pMDLg/RRE (Addgene #12251): encoding the gag and pol coding sequences and HIV-1 Responsive element (RRE)
- pRSV-REV (Addgene #12253): encoding HIV-1 Rev shuttle protein
- pBA571(Addgene #85968): containing 18 nucleotides-long barcode, BFP sequence and PuroR gene

3.6.2 Packaging plasmid DNA amplification and purification (maxiprep)

Top10 competent cells were used for packaging plasmid production. For the transformation, 100 ng (2 µl) of plasmid were added to the cells and the mixture was placed on ice for 2 min, then heat-shocked at 42 °C for 45 seconds, and then put back on the ice for an additional 2 min. Luria-Bertani (LB) medium (250 µl) was added to the mix and cells were incubated for 20-30 min at 37 °C, shaking at 180 rpm. 50 µl of the solution was spread on LB agar plates with a selection antibiotic and the cells were left to grow overnight. The

next morning, single colonies were selected, put in 3 ml of LB medium with ampicillin (500x), and left shaking at 180 rpm at 37 °C for 8 hours. After incubation,1 ml of the pre-culture was transferred to 500 ml of LB medium with ampicillin (500x) and left shaking at 180 rpm at 37 °C overnight. NucleoBond® Xtra Maxi kit (MACHEREY-NAGEL) was used for plasmid DNA purification from bacterial cultures according to the manufacturer's instructions. Cells were resuspended, lysed, and subsequently neutralized with appropriate buffers. Lysates, containing the plasmid DNA, were then transferred to a NucleoBond® Xtra Column, included in the kit, and cleared by the specially designed column filter. Next, plasmid DNA was bound to the NucleoBond® Xtra Silica Resin and, after a washing step, eluted in a high-salt concentration buffer. DNA was precipitated with the addition of isopropanol and the pellet re-dissolved in a low volume of dH_2O. Finally, purified plasmids were quantified on the NanoDrop 1,000 spectrophotometer (Thermo Scientific).

3.6.3 Transient transfection of 293T cells

To produce GBC libraries, a modified Packaging protocol for pooled lentiviral shRNA libraries (Cellecta) was used, adapted for 3rd generation vectors and 10 cm plates. Low passage 293 T cells were seeded in 10 cm plates to obtain sub-confluent (70-80%) cultures. Cells were kept in DMEM media supplemented with glutamine and 10% FBS without antibiotics. For each 10 cm plate the following mixes were prepared:

Mix1:

- pMD2.G VSV.G: 3 µg
- pMDLg/RRE: 6 µg
- pRSV-REV: 4 µg
- pBA571: 2.66 µg
- PlusTM Reagent 26.6 µl
- DMEM 533 µl

Mix 2

- LipofectamineTM 40 µl
- DMEM 533 µl

Mix 1 and Mix 2 were incubated for 15 minutes at room temperature, and then mixed, and incubated for another 15 minutes at room temperature. The mix was then added to the cells, which were then incubated at 37 °C for 24 hours. The virus was collected 24 and 48 hours later, filtered through a 0.22 µl filter unit, and concentrated 1,000x by

ultracentrifugation at 53,550 x g, for 2 hours at 16 °C. Virus was then diluted in PBS and stored at -80 °C.

3.6.4 Virus titration

To determine the virus titer, 293T cells were infected with serial dilutions of the frozen virus stock. Cells were plated at a concentration of 2 x 10^5 cells/ ml in 1 ml of medium per well in a 12-well plate. Amounts of virus added were 1 µl, 0.1 µl, 0.01 µl, 0.001 µl, and 0.0001 µl (in duplicates). Cells were collected 72 hours after infection, fixed with 4% PFA, washed, and resuspended in PBS for FACS acquisition. Titer was calculated by the following formula, taking into consideration virus dilutions that infected between 1% and 20% of the cells:

$$Viral\,Titer\left(\frac{particles}{\mu l}\right) = \frac{Number\ of\ plated\ cells \cdot \%\ of\ infected\ cells}{Volume\ of\ viral\ suspension(\mu l)}$$

3.6.5 Infection of human AML PDX models

Freshly isolated AML cells were plated at a density of 10^6 cells per ml in a 24-well plate precoated with Retronectin (Takara Bio). AML culture media was supplemented with polybrene (Sigma) at a final concentration of 8 µg/ml. 2 million viral particles were added per well to achieve an MOI 2 which ensures a good infection efficiency within the limits of the single-integration per cell requirement for clonal tracking experiments. The spin infection was performed at 435 x g, 45 min, room temperature (RT), after which cells were left to incubate for 16 hours. After incubation, half of the cells (5 x 10^5 cells) were transplanted into NSG mice, while the other half was frozen for DNA sequencing as a reference sample.

3.7 Single-cell RNA sequencing (scRNAseq)

3.7.1 Sample preparation for scRNAseq

Some samples were submitted as bulk population, while some were sorted for subpopulations (GFP-high, -low, -neg). After sorting, samples were counted and resuspended in 100 µl of 0.04 % bovine serum albumin in PBS (BSA/PBS), centrifuged, the supernatant was removed and cells were resuspended in an appropriate volume of 0.04 % BSA/PBS (volume was decided based on the target number of cells to be sequenced and the corresponding optimal concentration of cells, based on 10x Genomics guidelines). Cells

were counted again, taking note of the percentage of alive cells, and submitted for sequencing.

3.7.2 Multiplexing by hashing

To overcome the obstacle of low cell number recovery from certain samples (e.g. post-chemotherapy), falling below the threshold of 800 cells provided by 10x Genomics, sample multiplexing was performed using molecular hashtags (TotalSeq-B anti-human hashtag antibody, Biolegend). This is a recently developed technology, which enables mixing multiple samples together and submitting them for sequencing, after which samples can be demultiplexed and each read is assigned to its respective sample. In detail, molecular hashtags (antibodies) for proteins ubiquitously expressed on human cells (β-2 microglobulin and CD 298) were used. Cells were, after blocking, resuspended in antibody mix and incubated for 30 min at 4 °C. Cells were then washed with PBS and counted, after which equal numbers of cells per sample were mixed with other samples and then submitted for scRNAseq.

3.7.3 Library preparation and sequencing

On average, 2,000-3,000 cells per sample were used for sequencing. Cells were processed and libraries were prepared with Chromium Single Cell 3' Reagent kit v2 (10x Genomics), Chromium Single Cell 3' Reagent kit v3 (10x Genomics), or Chromium Next GEM Single Cell 3' Reagent kit v3.1 (10x Genomics). Paired-end sequencing at high coverage (50,000 reads per cell) was performed on Illumina NovaSeq 6000 platform.

3.7.4 GBC library barcode amplification

Barcode amplification was required as an additional step for the clonal tracking analysis with the GBC library. A small aliquot of the cDNA PCR2 product prepared with the Chromium Single Cell 3' Reagent kits was used for this purpose. PCR1 product of the Chromium Single Cell 3' Reagent kits protocol contained the barcoded (10xBarcode, unique molecular identifier), full-length cDNA, attached to Illumina TruSeq Read1 and poly(dT) sequence while PCR2 product contained also Illumina TruSeq Read2 and P5 and P7 adaptors used in Illumina bridge amplification. Barcode enrichment was then used to specifically amplify barcode sequences. The amplified barcodes were then mixed with their respective samples and scRNAseq was performed. To perform barcode amplification, two rounds of

PCR were performed, using semi-nested primers, which contained sequences complementary to the immobilized primers necessary to initiate amplification in the Illumina NovaSeq 6000 platform (Table 4).

Table 4. Primers used for barcode amplification and sequencing

Application	Round	Name	Sequence
Barcode amplification	1st	FWTTA5	AATGATACGGCGACCACCGAGATCTAC ACATAGATGCTCACACTCTTTCCCTACA CGACGCTCTTCCGATCT
		FWTTA6	AATGATACGGCGACCACCGAGATCTAC ACGAAGTTAGGGACACTCTTTCCCTAC ACGACGCTCTTCCGATCT
		FWTTA7	AATGATACGGCGACCACCGAGATCTAC ACAAAGGTAGTAACACTCTTTCCCTAC ACGACGCTCTTCCGATCT
		Reverse_SI-GA-G3	CAAGCAGAAGACGGCATACGAGATGA ATGAGGGTGACTGGAGTTCAGACGTGT GCTCTTCCGATCTTAGCAAAACTGGGG CACAAGE
	2nd	FWTTA5	AATGATACGGCGACCACCGAGATCTAC ACATAGATGCTCACACTCTTTCCCTACA CGACGCTCTTCCGATCT
		FWTTA6	AATGATACGGCGACCACCGAGATCTAC ACGAAGTTAGGGACACTCTTTCCCTAC ACGACGCTCTTCCGATCT
		FWTTA7	AATGATACGGCGACCACCGAGATCTAC ACAAAGGTAGTAACACTCTTTCCCTAC ACGACGCTCTTCCGATCT
		RVTA5	CAAGCAGAAGACGGCATACGAGATGTA GCCCTGTGTGACTGGAGTTCAGACGTG TGCTCTTCCGATCTTAGCAAACTGGGGC ACAAGC
		RVTTA6	CAAGCAGAAGACGGCATACGAGATTAA CGCGTGAGTGACTGGAGTTCAGACGTG

			TGCTCTTCCGATCTTAGCAAACTGGGGC ACAAGC
		RVTTA7	CAAGCAGAAGACGGCATACGAGATTCC CAAGGGTGTGACTGGAGTTCAGACGTG TGCTCTTCCGATCTTAGCAAACTGGGGC ACAAGC
Sequencing		PE Read 1 Sequencing Primer	ACACTCTTTCCCTACACGACGCTCTTCC GATCT
		PE Read 2 Sequencing Primer	CGGTCTCGGCATTCCTGCTGAACCGCTC TTCCGATCT

The first round of PCR served to specifically select barcode sequences and distinguish them from genomic DNA, and to replace adaptor sequences at the ends of each read. Primers used for the first round of PCR contained the P5 (FWTTA5, FWTTA6, FWTTA7) and P7 (Reverse_SI-GA-G3) adaptor sequences for the Illumina flow cell. For the first round of PCR, 5 ng of cDNA was used and a master mix was prepared as described in table 5 below, while thermocycling conditions are reported in table 6.

Table 5. Master mix preparation for PCR1

Component	Concentration
NEBNext® Ultra™ II Q5® Master Mix	2x
FW primer (10 µM)	0.125 µM
RV primer (10 µM)	0.125 µM
cDNA	5ng
dH2O	(to 30 µl)

Table 6. Thermocycling conditions for PCR round 1

Process	Temperature	Time	Cycles
Initial denaturation	98	10 sec	1
Denaturation	98	5 sec	22
Annealing	72	5 sec	
Extension	72	10 sec	
Final extension	72	1 min	1

After the first round of PCR, 10 µl of each sample was analyzed by gel-electrophoresis in order to check if amplicons were of the correct size. Samples were loaded on a 2% agarose gel 1X TAE (1X Tris-acetate-EDTA buffer) and run until amplicon bands were well visible. Following that, samples were diluted 3,000x and 2 µl of diluted sample was used as template for the second round of PCR. The second PCR round has been designed to specifically select for amplified barcode DNA and discard non-specific PCR products. The primers used for this second amplification contained the double index sequences used for the Illumina sequencing. Master mix for the second round PCR was prepared as described below (Table 7) and thermocycling conditions are described in the Table 8.

Table 7. Master mix preparation for PCR2

Component	Concentration
NEBNext® Ultra™ II Q5® Master Mix	2x
FW primer (10 µM)	0.125 µM
RV primer (10 µM)	0.125 µM
cDNA	2 µl of diluted PCR1 product
dH2O	(to 30 µl)

Table 8. Thermocycling conditions for PCR round 2

Process	Temperature	Time	Cycles
Initial denaturation	98	10 sec	1
Denaturation	98	5 sec	20
Annealing	72	5 sec	
Extension	72	10 sec	
Final extension	72	1 min	1

After the second round of PCR, samples were analyzed by gel-electrophoresis in order to check if amplicons were of the correct size. Samples were loaded on a 2% agarose gel 1X TAE (1X Tris-acetate-EDTA buffer) and run until amplicon bands were well visible. PCR products were then purified using the QIAquick PCR purification kit (QIAGEN), according to instructions given by manufacturer. In detail, samples were mixed with high-salt binding buffer, which enables the binding of DNA to silica membrane, while other

ingredients, like primers, nucleotides, enzymes, salts, agarose and others, were removed by centrifugation. At the end, DNA was eluted from the silica membrane in a low (30-50 µl volume of water in order to keep the DNA concentrated. DNA quantification was performed on Nanodrop or Qubit.

3.8 GBC library genomic DNA processing

GBC library genomic DNA was used to define the list of GBC barcodes found in each sample, which served as a reference for the analysis of transcriptional profiles of GBC clones. Genomic DNA was extracted from both reference samples (mentioned above §3.6.5) taken at the time of transplantation, as well as BM and PB samples. Spike-in controls (section 3.7.1) were used to assign cell number to read number ratio for each sample.

3.8.1 Spike-in preparation

Separate preparations of Perturb-seq plasmids carrying single barcodes were used to produce virus and to infect NB4 cells. Cells were plated at a density of 5 x 10^5 cells per ml in media supplemented with 8 µg/ml polybrene and infected with variable MOIs (0.2- 1). Spin infection was performed at 435 x g, 45 min, RT, followed by 16 hours of incubation, after which media was changed and cells were left in a humidified incubator for another 72 hours, to allow for BFP expression. Infected cells were then sorted as BFP+, and aliquots containing predefined numbers of cells were prepared. Different spike-in controls were used to prepare aliquots of 10, 10^2, 10^3, 10^4, 5 x 10^4, 10^5 and 10^6 cells, each of them labeled with a unique barcode. Based on sample cellularity and the expected barcode distribution, an appropriate set of spike-in controls was added to each sample before DNA extraction.

3.8.2 DNA extraction

Cells were resuspended in lysis buffer (10 mM Tris-Cl pH 8.0, 0.5 mM EDTA, 0.2% SDS, 100mM NaCl and 0.1mg/ml proteinase K) and incubated overnight at 55 °C. Temperature was increased to 80 °C for 30min to inactivate proteinase K. Samples were then mixed with 1 volume of isopropanol in order to precipitate DNA and centrifuged at maximum speed (16,000 x g) for 1 hour at 4 °C. Pellets were then washed with 70% ethanol and left to dry. Dry pellets were resuspended in 20 µl of dH_2O, and placed in thermomixer, shaking at 1,000 rpm, RT for 30 min for better rehydration. Quantification was performed on Nanodrop or Qubit.

3.8.3 Barcode amplification from genomic DNA

For barcode amplification up to 250 ng of genomic DNA was used as template for a single round of PCR. In case of non-specific amplification (observed after agarose gel-electrophoresis or a Bioanalyzer run), a second round of PCR can be performed. Primers used are shown on table 9 below. Master mix specifications and thermocycling conditions are shown on tables 10 and 11.

Table 9. Primers used for barcode amplification and sequencing

Application	Name	Sequence
Barcode amplification	F1	GGGTTTAAACGGGCCCTCTA
	R2	GGGAGCCATCTGATCGCAAA
Sequencing	PE Read 1 Sequencing Primer	ACACTCTTTCCCTACACGACG CTCTTCCGATCT
	PE Read 2 Sequencing Primer	CGGTCTCGGCATTCCTGCTGA ACCGCTCTTCCGATCT

Table 10. Master mix preparation for PCR1

Component	Concentration
NEBNext® Ultra™ II Q5® Master Mix	2x
F1new(10 μM)	0.125 μM
R2new (10 μM)	0.125 μM
DNA template	200-300 ng
dH2O	(to 15 μl)

Table 11. Thermocycling conditions for PCR round 1

Process	Temperature	Time	Cycles
Initial denaturation	98	30 sec	1
Denaturation	98	7 sec	30
Annealing	64	25 sec	
Extension	72	15 sec	
Final extension	72	1 min	1

In samples which had low DNA concentration, total DNA was split in 2 reactions. After the first round of PCR, all reactions per sample were mixed, and 10 μl of each sample was analyzed by gel-electrophoresis in order to check if amplicons are of the correct size. Samples were loaded on 2% agarose gel 1X TAE (1X Tris-acetate-EDTA buffer) and run until amplicon bands were well visible. PCR products were then purified using QIAquick PCR purification kit (QIAGEN), according to instructions given by manufacturer. In detail, samples were mixed with high-salt binding buffer, which enable binding of DNA to silica membrane, while other ingredients, like primers, nucleotides, enzymes, salts, agarose and other, are removed by centrifugation. In the end, DNA was detached from silica membrane by the addition of low-salt elution buffer or water. A small elution volume (30-50 μl) was used in order to keep the DNA content concentrated. DNA quantification was performed on Nanodrop or Qubit. Finally, the presence of a single 240bp band was confirmed on the Bioanalyzer (Agilent).

3.8.4 DNA sequencing

On average, 1-5 ng of amplicon DNA per sample were used for library preparation following the HT-ChIP-Seq Library preparation protocol. Paired-end sequencing with high coverage (30 x 10^6 reads per sample) was performed on the NovaSeq 6000 platform.

3.8.5 Barcode distribution analysis

The first step was to distinguish real barcode sequences from barcode sequences which were found as a consequence of sequencing error. 93% of total reads was selected as real barcodes, while 7% was excluded. This percentage was selected empirically, based on the expected numbers of barcodes in samples and references. We then used the number of cells that supported any GBC to derive the relative frequency of that GBC in the population. The relative frequencies were binned, and the binning size was determined by taking advantage of the Freedman-Diaconis rule as:

$$Binning\ size = 2 \cdot \frac{IQR}{\sqrt[3]{n}}$$

where IQR is the interquartile range of relative frequencies and n is the total number of different GBCs. We determined the number of GBCs that belonged to each bin and derived the distribution of GBCs in bins.

3.9 Statistical analysis

Data are represented as average ± standard deviation. All statistical tests are reported in the legend of each figure and the corresponding p-values are reported in the legend of each figure or on the figure itself.

Shannon Entropy was used to calculate the complexity of a clonal population. For any given sample j, the formula for Shannon Entropy is:

$$SH_j = -\sum_{i=1}^{N} p_i \cdot \log(p_i)$$

where pi is the frequency of the observation i in a sample composed of N observations.

Expansion index was calculated as (1 – Shannon Equitability). Shannon Equitability represents the value of Shannon Entropy (for a given sample) divided by the maximum value that Shannon Entropy can have. Expansion index was used to compute the clonality of a given sample. In particular, for any given sample j, the formula for the expansion index is:

$$Expansion\ index_j = 1 - \frac{-\sum_{i=1}^{N} p_i \cdot \log(p_i)}{logN}$$

where N is the number of observations in the sample j. This index ranges from 0 to 1, where 1 corresponds to a purely monoclonal sample (i.e., N = 1 and pi = 1) and 0 corresponds to a sample composed of N observations with uniform frequency.

To understand which clusters are expanded/depleted in different samples (e.g. before and after chemotherapy), we divided the relative fraction of the cluster in the sample of interest by the relative fraction of the cluster in the baseline sample. Following that log2 fold change (LOG2FC) was calculated from these values. Clusters with positive LOG2FC values were considered as enriched, while clusters with negative LOG2FC values were considered as depleted in the sample of interest.